Available online at www.sciencedirect.com
ScienceDirect
International Journal of Mass Spectrometry 268 (2007) 265–276
International Journal of Mass Spectrometry
www.elsevier.com/locate/ijms

The saliva proteome of the blood-feeding insect *Triatoma infestans* is rich in platelet-aggregation inhibitors

Sébastien Charneau [a,1], Magno Junqueira [b,1], Camila M. Costa [a], Daniele L. Pires [c], Ellen S. Fernandes [c], Ana C. Bussacos [c], Marcelo V. Sousa [a,*], Carlos André O. Ricart [a], Andrej Shevchenko [b], Antonio R.L. Teixeira [c]

[a] *Laboratory of Biochemistry and Protein Chemistry, Department of Cell Biology, University of Brasília, Brasilia 70910-900-DF, Brazil*
[b] *Max Planck Institute of Molecular Cell Biology and Genetics, Pfotenhauerstrasse 108, 01307 Dresden, Germany*
[c] *Chagas Disease Multidisciplinary Research Laboratory, Faculty of Medicine, University of Brasília, Brasilia 70910-900-DF, Brazil*

Received 1 March 2007; received in revised form 3 May 2007; accepted 8 May 2007
Available online 16 May 2007

Abstract

The saliva of the bloodsucking bug *Triatoma infestans* vector of Chagas disease contains an anti-hemostatic molecular cocktail that prevents coagulation, vasoconstriction and platelet aggregation in a vertebrate prey. In order to characterize *T. infestans* saliva proteome, we separated the secreted saliva by two-dimensional gel electrophoresis (2-DE). More than 200 salivary proteins were detected on the 2-DE map, mainly in the alkaline region. By nanoLC–MS/MS analysis using a LTQ–Orbitrap equipment followed by a combination of conventional and sequence-similarity searches, we identified 58 main protein spots. Most of such proteins possess potential blood-feeding associated functions, particularly anti-platelet aggregation proteins belonging to lipocalin and apyrase families. The saliva protein composition indicates a highly specific molecular mechanism of early response to platelet aggregation. This first proteome analysis of the *T. infestans* secreted saliva provides a basis for a better understanding of this fluid protein composition highly directed to counterpart hemostasis of the prey, thus promoting the bug's blood-feeding.

Keywords: *Triatoma infestans*; Saliva proteomic; Chagas disease; Tandem mass spectrometry; Sequence-similarity search

1. Introduction

Chagas disease, one of the most devastating parasitic human infections, is wide spread in South America. It was estimated at 16–18 million people infected by the protozoan *Trypanosoma cruzi*, with an annual death rate of 50,000 cases [1,2]. The disease is transmitted during blood-feeding of triatomine bug (Hemiptera: Reduviidae; Triatominae) vectors, which release the parasite in the feces, infecting human through skin lesions.

The first line of vertebrate defense against blood loss is platelet aggregation that forms a hemostatic plug. Platelet aggregation is accomplished through a biochemical cascade triggered by collagen, thrombin, thromboxane A2 and ADP [3,4]. To preserve host blood flow during feeding, saliva of hematophagous insects contain platelet-aggregation inhibitors.

Triatoma infestans is considered a main vector in the epidemiology of Chagas disease in some ecosystems of South America, because it feeds more efficiently than its *Triatominae* competitors [5,6]. Several salivary proteins of triatomine bugs have been characterized so far, the majority consisting of platelet inhibitors. Two *T. infestans* salivary proteins, triplatin-1 and -2, inhibit platelet aggregation induced by collagen, but not by ADP or thrombin [7]. *Triatoma pallidipennis* saliva contains two inhibitors of platelet aggregation, pallidipin, which shares function and sequence similarities with triplatins [8] and triabin, a thrombin-induced platelet-aggregation inhibitor [9,10]. Another platelet-aggregation inhibitor from triatomine bugs is the *Rhodnius prolixus* ADP-binding protein *Rhodnius* Platelet Aggregation Inhibitor 1 (RPAI1) [11] that inhibits ADP-induced platelet aggregation [12]. Triplatin, pallidipin, triabin and RPAI, all belong to the family of lipocalins that are extracellular

Abbreviations: IEF, isoelectric focusing; IPG, immobilized pH gradient; 2-DE, two-dimensional gel electrophoresis; MS BLAST, mass spectrometry driven BLAST; TiAPY, *Triatoma infestans* apyrase; DTT, dithiothreitol

* Corresponding author. Tel.: +55 61 3307 2142; fax: +55 61 3273 4608.
E-mail address: mvsousa@unb.br (M.V. Sousa).
[1] These authors contributed equally for this work.

1387-3806/$ – see front matter © 2007 Elsevier B.V. All rights reserved.
doi:10.1016/j.ijms.2007.05.004

transport proteins [13]. In *R. prolixus* saliva, the strongest anti-platelet aggregation activity triggered by ADP is attributed to apyrase, a nucleoside triphosphate-diphosphohydrolase that hydrolyses ATP or ADP to AMP [14,15]. This *R. prolixus* enzyme has not been isolated yet and, like other apyrases, does not belong to the lipocalin family.

T. infestans saliva also manifests salivary apyrase activity [16]. It appears that *T. infestans* salivary apyrases play an important role in the insect feeding habit, and half of its storage is used during single blood meal [17]. It has been shown that the apyrase activity of *T. infestans* saliva should be related to five glycosylated proteins with apparent molecular masses of 88, 82, 79, 68 and 67 kDa, that can not be distinguished by non-denaturing one-dimensional gel electrophoresis due to homo-oligomerization [18]. Only the full sequence of the *Tiapy79* gene encoding the 79 kDa apyrase was reported, confirming that it belongs to the 5′-nucleotidase family [16].

Despite of the medical importance of *T. infestans* vectoring, relatively little is known about its genome. Currently, sequences of 35 *T. infestans* proteins are available in NCBI database. Therefore, proteomics efforts utilizing conventional database searching approaches that rely on exact correlations of masses of intact peptides (in peptide mass fingerprinting) or masses of precursors and fragments (in tandem mass spectrometry) to corresponding database entries were expected to deliver limited identification efficiency (reviewed in [19]). The identification could rely on cross-species matching of spectra from *Triatoma* peptides to identical peptide sequences in known homologous proteins. Alternatively, unmatched peptide spectra could be completely or partially interpreted de novo (reviewed in [20]) and obtained sequence candidates used in error-tolerant searches (reviewed in [21]). Both stringent and error-tolerant approaches can be combined in a layered fashion such that, first, the known and highly homologous proteins are identified in stringent cross-species searches, and then the rest of spectra is interpreted de novo and complete or partial peptide sequences are applied for similarity driven identifications [22,23]. The former approach is considerably faster since it utilizes uninterpreted tandem mass spectra, however it typically produces hits with only a few matched peptides and therefore their statistical confidence could be compromised. The sequence similarity approach is more challenging technically, however, by tolerating multiple mismatches in aligned peptide sequences, it almost doubles the number of identified proteins [23–26].

Mass spectrometry-based strategy has been used for characterizing the proteome of salivary gland from *Anopheles gambiae*, the major malaria vector. That study provided validation for the existing genome annotation, and also discovered novel proteins, which had been represented only as predicted transcripts in the databases and not previously identified as cDNAs [27]. This illustrates the complementary nature of different strategies for identification of gene products.

Herein, we present the first proteomic study of the *T. infestans* saliva. 2-DE maps revealed more than 200 salivary protein spots, most of them in the alkaline pH range. The majority of proteins identified by mass spectrometry is potentially engaged in platelet-aggregation inhibition and belongs to triabin subfamily and apyrase family. The results also revealed that several proteins were present in multiple isoforms having partial sequence redundancy.

2. Materials and methods

2.1. Harvest of triatomine saliva

T. infestans colony was reared in the insectarium of the Chagas Disease Multidisciplinary Research Laboratory, University of Brasília, maintained at 28 °C, 70% relative humidity, with photoperiods of 12 h. Secreted *T. infestans* saliva was collected by using pipette tips placed in contact with the insect mouthparts at 7–9 days following the blood meal. Protease Inhibitor Mix without EDTA (GE Healthcare, Uppsala, Sweden) was added to the saliva and samples stored at −80 °C. For tissue localization experiments, saliva samples were extracted from the salivary glands D1, D2 and D3. Glands in 0.9% saline solution were carefully punctured with a needle, and extracted intra-luminal saliva was harvested by centrifugation.

2.2. Quantification of sample

Samples of pooled saliva obtained from several adult insects, were quantified using the Plus One 2D Quant Kit (GE Healthcare) and, in parallel, by amino acid analysis on a Hitachi L8500 amino acid analyzer using ninhydrin post-column derivatization.

2.3. Two-dimensional gel electrophoresis

2.3.1. Wide pH range

T. infestans saliva samples containing 80 or 300 μg protein were diluted and incubated for 1 h at room temperature in 350 μL final volume of denaturing sample buffer containing 7 M urea, 2 M thiourea, 66 mM DTT, 2% Triton X-100, 0.5% Pharmalyte 3–10, and 10% isopropanol. Samples were centrifuged (12,000 × *g*, 10 min) prior to IEF.

The supernatants were applied to 18 cm IPG gel-strips with linear separation pH range of 3–10 (GE Healthcare) by in-gel rehydration [28] for 6 h without current followed by 6 h at 30 V. IEF was carried out at 20 °C using an Ettan IPGphor3 unit (GE Healthcare) with the following conditions, 500 V for 1 h, 1000 V for 1 h and 8000 V for 4 h with a maximum current of 50 μA per strip. Prior to SDS-PAGE, the IPG strips were subjected to reduction with equilibration buffer (50 mM Tris, pH 8.8, 6 M urea, 30% glycerol, 4% SDS) supplemented with 125 mM DTT for 40 min and alkylation with 300 mM acrylamide in equilibration buffer for additional 40 min. SDS-PAGE was performed on 12% T polyacrylamide gels run on a Protean II system (Bio-Rad, Richmond, CA, USA) at 20 °C. Proteins were visualized by silver staining [29] and the gels were stored in 1% acetic acid before protein digestion. Alternatively, the 2-DE gels were submitted to Western blotting.

2.3.2. Basic pH range

IPG gel-strips of 11 cm with a linear separation alkaline pH window of 6–11 were rehydrated in 200 μL of denaturing sam-

ple buffer containing 10% isopropanol for 10 h. *T. infestans* saliva (240 μg proteins) was diluted and incubated for 1 h at room temperature in 200 μL final volume of denaturing sample buffer containing 10% isopropanol. The samples were centrifuged (12,000 × *g*, 10 min) and applied to a paper bridge, a small piece of CleanGel electrode strip paper (Amersham 18-1035-33), according to Ref. [30] positioned at the anode of the Multiphor II apparatus (Amersham Biosciences) and an electrode pad embedded in DTT solution was positioned near the cathode. IEF was carried out at 20 °C with the following conditions: 150 V for 1 h, 300 V for 1 h, 600 V for 1 h and 3500 V for 5 h, under a current of 2 mA. For the second dimension, reduction and alkylation of the IPG strips were carried out as described above. SDS-PAGE was performed on 10% T polyacrylamide gels run on a SE 600 Electrophoresis Unit (Hoefer) at 20 °C. Gels were then either silver-stained and stored in 1% acetic acid before protein digestion or submitted to Western blotting.

2.4. Raising antisera against T. infestans apyrases

T. infestans salivary proteins were separated by 10% SDS-PAGE and visualized by Coomassie blue staining. The gel bands corresponding to 88, 82 and 79 kDa apyrases were excised independently, macerated and solubilized in 200 μL of Tris-buffered saline (TBS).

Polyclonal antisera against such apyrases were raised by immunizing rabbits with 5 μg of each form per injection (first injection with complete Freund's adjuvant, second injection with incomplete Freund's adjuvant and third injection without adjuvant). Sera were collected, diluted with one volume of glycerol and stored at −20 °C.

2.5. Immunoblotting

Saliva proteins, separated by SDS-PAGE or 2-DE were electroblotted onto nitrocellulose membrane (Hybond-C Extra, Amersham Biosciences) using a Trans-Blot Electrophoretic Transfer Cell (Bio-Rad). The membrane was blocked with 5% non-fat milk and 0.1% Tween 20 in TBS for 1 h at room temperature followed by incubation for 2 h with anti-apyrase rabbit serum, diluted to 1:200 in 1% non-fat milk in TBS. After three washes in TBS, the membrane was incubated with alkaline phosphatase-conjugated anti-rabbit IgG for 1 h, washed extensively in TBS and revealed using 5-bromo-4-chloro-3-indolyl-1-phosphate and nitro blue tetrazolium (Bio-Rad) as substrates.

2.6. Image analysis

Silver-stained gels were scanned with a Sharp JX-330 scanner at 300 dpi resolution. Digitized images were analyzed with Image Master 2D Elite software (Amersham Biosciences) to match and quantify protein spots.

2.7. Protein identification by nanoLC–MS/MS

Protein spots were excised from silver-stained gels, and in-gel digested with trypsin as described in Ref. [31]. Recovered peptides were analyzed by nanoLC–MS/MS on an Ultimate 3000 system (Dionex, Amsterdam, The Netherlands) interfaced online with a LTQ–Orbitrap mass spectrometer (ThermoFisher Scientific., San Jose, CA). To this end, peptides were redissolved in 0.05% TFA and loaded onto 5 mm × 300 μm i.d. trapping microcolumn packed with C18 PepMAP100 5 μm particles (Dionex) in 0.05% TFA at the flow rate of 20 μL/min. Upon loading and washing, peptides were back-flush eluted onto a 15 cm × 75 μm i.d. nanocolumn, packed with C18 PepMAP100 3 μm particles (Dionex). The following mobile phase gradient was delivered at the flow rate of 200 nL/min: 5–20% of solvent B in 20 min; 20–50% B in 16 min; 50–100% B in 5 min; 100% B during 10 min, and back to 5% B in 5 min. Solvent A was 95:5 H_2O/acetonitrile (v/v) with 0.1% formic acid and solvent B was 20:80 H_2O/acetonitrile (v/v) with 0.1% formic acid. Peptides were infused into the mass spectrometer via dynamic nanospray probe (ThermoElectron Corp.) with 10 μm i.d. SilicaTip uncoated needle (New Objective, Woburn, MA). The spray voltage was set to 1.8 kV with no sheath and auxiliary gas flow; ion transfer tube temperature was 180 °C. Mass spectrometer was operated in data-dependent mode. The automated gain control (AGC) was set to 5×10^5 charges and 5×10^4 charges for MS/MS at the linear ion trap analyzer. DDA cycle consisted of the survey scan within *m*/*z* 300–1600 at the Orbitrap analyzer with target mass resolution of 60,000 (FWHM, full width at half maximum) followed by MS/MS fragmentation of the four most intense precursor ions under the relative collision energy of 35% in the linear trap. Singly charged ions were excluded from MS/MS experiments, and *m*/*z* of fragmented precursor ions were dynamically excluded for further 90 s. Ion selection threshold for triggering MS/MS experiments set to 500 counts. An activation parameter *q* 0.25 and activation time of 30 ms were applied. The entire pool of dta files was converted into a single mgf (MASCOT generic format) file using BioWorks 3.2 software (Thermo Electron Corp.) and searched against MSDB database by MASCOT v. 2.1 software (Matrix Science Ltd., London, U.K.) installed on a local 2 CPU server. Database searching settings were mass tolerance of precursor ions of 10 ppm and an fragment ions of 0.8 Da; up to two missed cleavages were allowed; carbamidomethylation of cysteine, oxidation of methionines and *N*-protein acetylation were set as variable modifications. The confidence criteria for protein identification by MASCOT were set conditionally on the number of matched peptides and also peptide ion scores of each individual match. First, no matched spectra with peptide ions scores below 20 were considered and, at least, three spectra should be matched. For hits identified with less than three matched spectra it was required that at least one spectrum was matched with the score of 50 or higher. Upon MASCOT searches, dta files corresponding to MASCOT hits (including keratin and trypsin peptides) were removed and the rest submitted to de novo interpretation by a modified version of PepNovo software in batch mode [32].

While interpreting each dta file, PepNovo produced up to seven redundant, degenerate and partially inaccurate sequence candidates. PepNovo assigned a quality score for each top candidate, which stands for the expected number of correctly

determined amino acid residues in the full peptide sequences. For subsequent sequence-similarity database searches, we only considered the candidates whose PepNovo quality score exceeded 6. All selected candidates were merged into MS BLAST query string as described in Refs. [23,33] and then submitted to MS BLAST searches against nr database at http://genetics.bwh.harvard.edu/msblast/. Statistical confidence of database searching hits was estimated according to MS BLAST scoring scheme [34], whoever hits related to trypsin and keratins were excluded and only high scoring segment pairs (HSP) with scores above 55 were considered.

2.8. Sequence and phylogenetic analysis

The unrooted tree was generated using the CLUSTALW multiple alignment program at http://www.ebi.ac.uk/clustalw/ using neighbor-joining method. Eight triabin-related proteins from lipocalin family of *T. infestans* were considered in building the alignments. The phylogenetic tree was formatted with TreeView software.

3. Results and discussion

3.1. Proteomic map of T. infestans saliva

Two-dimensional electrophoresis analysis of *T. infestans* saliva was initially performed using isoelectric focusing within a wide pH range (3–10). Since most protein spots were found in the alkaline region of the gel, we optimized IEF conditions to improve the detection of basic polypeptides. Adding isopropanol to the sample buffer as well as gel rehydration under low voltage minimized protein precipitation and aggregation, which are more frequently observed in the alkaline region. In our conditions of insect rearing and saliva harvest, one bug produced about 1 μL of saliva, which corresponds to approximately 50 μg protein. Amounts equivalent to 80 and 300 μg saliva protein were loaded on separate gels. Upon 80 μg loading, we observed 204 silver-stained spots (Fig. 1A) versus 269 spots observed upon loading of 300 μg protein (Fig. 1B). The spots at molecular masses above 45 kDa were mostly detected in the basic region, and were not well resolved due to horizontal streaking (Fig. 1). The resolution of these high molecular mass spots was subsequently improved by using 6–11 pH gradient in the IEF step (see below).

Forty-three protein spots below 45 kDa were chosen for the identification as they were fairly well focused and represented all protein spot clusters scattered over the 2-DE gels (Fig. 1A and B). To this end, we applied tandem mass spectrometry, which is the most adequate strategy for protein identification when working with organisms lacking extensive genomic data as the *Triatoma* genus.

Thus, recovered peptides of in-gel tryptic digests from excised protein spots were subjected to analysis by nanoLC–MS/MS on a LTQ–Orbitrap mass spectrometer. Database mining was performed in a layered approach, first starting with stringent MASCOT database searches and followed by de novo interpretation of unassigned spectra and MS BLAST sequence-similarity searches with deduced sequence candidates. To this end, the entire pool of produced tandem mass spectra (typically, >4000 per run) was converted into a single mgf file

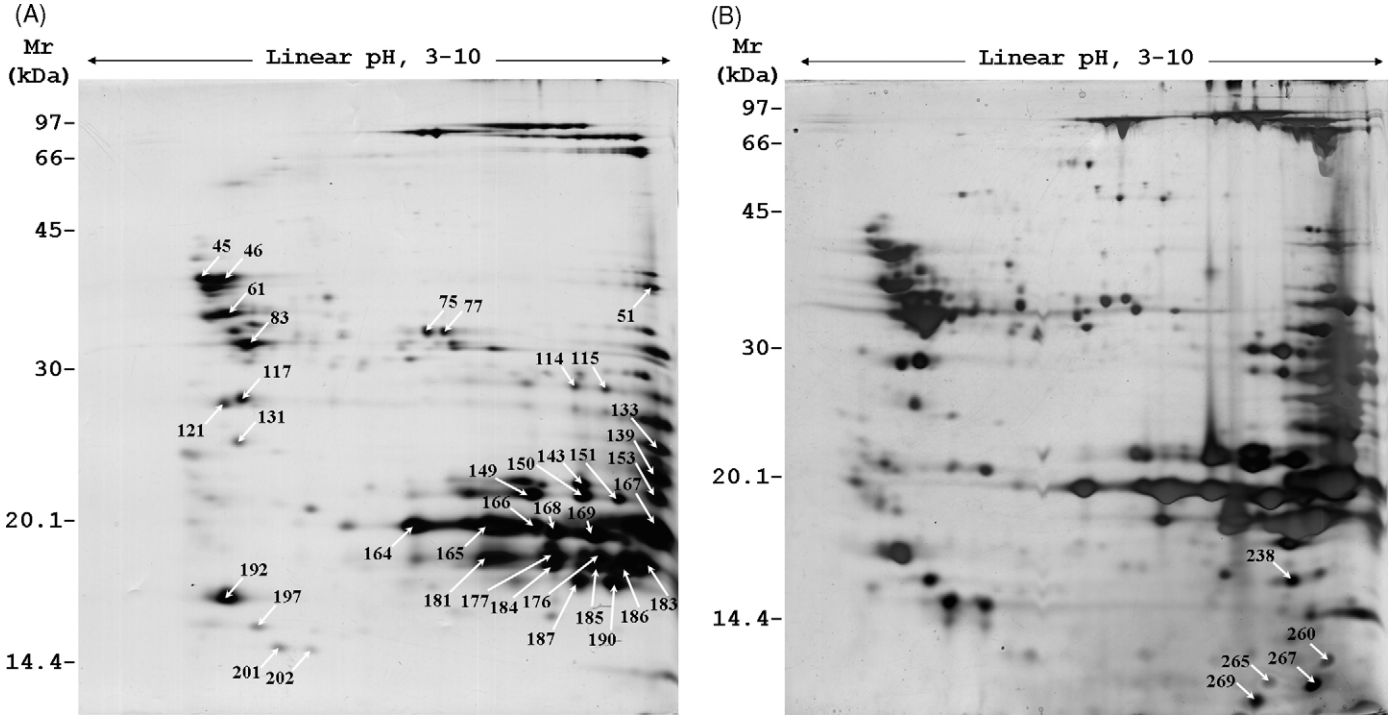

Fig. 1. Wide pH range 2-DE map of *T. infestans* salivary secreted proteins. 2-DE was performed under denaturing conditions using 3–10 linear IPG strip in IEF and 12% SDS-PAGE in second dimension. Sample amounts were 80 μg (A) and 300 μg (B). The gels were silver-stained. Spot numbers correspond to MS/MS identified proteins shown in Table 1.

and searched by MASCOT. Dta files corresponding to confident proteins hits were removed from the query and the rest was interpreted de novo by PepNovo software and obtained sequences used for MS BLAST searches. Altogether, among 43 attempted samples, MASCOT confidently identified 34 individual proteins. Applying sequence-similarity searches to the complete nanoLC–MS/MS dataset enabled us to identify another 11 proteins and to support previous cross-species identifications by MASCOT by error-tolerant matching of several new peptides in 23 cases. Whenever MASCOT and MS BLAST matched apparently different proteins, BLAST-P searches with full-length sequences of the corresponding database entries validated that these proteins were not homologous. Interestingly, in 10 spots we identified more than one unique protein, which is not uncommon considering the high dynamic range of nanoLC–MS/MS technique [35].

We grouped the identified salivary protein into three categories according to their assumed salivary function: (i) proteins with unknown function or non-identified, (ii) proteins with putative blood-feeding function and (iii) proteins with blood-feeding known function (Table 1 and Supplementary Table 1).

3.1.1. T. infestans salivary proteins with unknown function and non-identified proteins

The sequences from three saliva proteins matched the translated sequence of a triatox gene from *T. infestans* (SwissProt/TrEMBL accession number Q45KX2) using stringent MASCOT search. In this particular case, MS BLAST searches did not provide any positive hit. Triatox shows no sequence similarity to proteins from other organisms and its function is still unknown. It is the first time that the product of the triatox gene was detected. The triatox-like proteins identified in the 2-DE maps may comprise a new class of *Triatoma* secreted salivary proteins.

Four spots (83, 201, 260 and 269) of *T. infestans* saliva could not be identified by nanoLC–MS/MS.

These seven protein spots found in the secreted saliva correspond to molecules probably implicated in blood-feeding.

3.1.2. T. infestans salivary proteins with blood-feeding putative functions

Among all protein spots identified, seven can be considered as novel *T. infestans* salivary proteins having sequence homologies with proteins from other organisms available in databases.

Six spots of *T. infestans* crude saliva share sequence similarities with ATPases and phosphate binding proteins. ATPases have many different cellular functions, but in salivary gland cDNA library studies from *R. prolixus* bug and *An. gambiae* and *Ædes ægypti* mosquitoes, both ATPase and phosphate binding protein genes are classified as possible housekeeping function genes involved in energy metabolism and transport [27,36,37].

Three protein spots matched to both alpha and beta subunits from the F_1 portion of the F_o/F_1 ATP synthase complex from bacteria and yeasts. These subunits were previously detected in 2-DE maps of female *Æ. ægypti* mosquito salivary glands [37]. When the F_1 portion is physically separated from the membrane F_o portion, F_1 is only capable of catalyzing ATP hydrolysis. ATP hydrolysis may play a role in blood-feeding mechanisms since recent studies have shown that ATP may synergize with ADP as a platelet-aggregating agent [38]. It is also possible that these salivary proteins could be involved in energy metabolism associated with protein synthesis and secretion (as proposed by [37]) promoting the blood-feeding or could act as inhibitors of immune-response since ATP is known to be a signal for neutrophil activation.

Moreover, three other protein spots matched preferentially with periplasmic phosphate binding proteins from bacteria. In the future, we intend to take a special attention to these putative transport proteins for inorganic phosphate to understand their presence and role in the secreted saliva.

One protein spot (51) identified only by MS BLAST search, but not by MASCOT, is a hydrolase similar to secreted alkaline phosphatase L from *Pseudomonas aeruginosa*. A secreted salivary alkaline phosphatase containing a signal peptide was previously found in the mosquito *Æ. aegypti*, but its blood-feeding function is not yet established [37]. Recently, it was proposed that an inositol polyphosphate 5-phosphatase from *R. prolixus* secreted saliva facilitates the ingestion of blood by reducing the concentration of phosphatidylinositol 4,5-bisphosphate and phosphatidylinositol 3,4,5-trisphosphate at the surface of platelets and inactivating these particles [39].

All proteins mentioned above are potentially intracellular. It was previously described that although all three *T. infestans* salivary glands present merocrine secretion (exocytosis of the saliva components into the lumen), occasionally, budding vesicles containing large volume of intracellular components are released in the lumen, corresponding to apocrine secretion [40]. Therefore, the presence of intracellular proteins in saliva proteome results from the physiological process of secretion.

3.1.3. T. infestans salivary proteins with known blood-feeding functions

Remarkably, 34 *T. infestans* salivary spots were related to bug proteins with already established blood-feeding function. Thirty-one spots with different p*I*s and apparent molecular masses, matched to just six *T. infestans* protein sequences belonging to lipocalin family, indicating the presence of polymorphic variants due to either sequence divergence or post-translation modifications. All these six lipocalin sequences contain a putative triabin domain, so that we classified them as members of the triabin subfamily. Lipocalins from arthropods bind low molecular mass ligands and inhibit platelet activity, vasoconstriction, inflammation and coagulation in vertebrates [41,42].

Phylogenetic analysis with all available sequences of *T. infestans* lipocalin-like proteins, including TiLipo33, TiLipo37, TiLipo39, TiLipo77, infestilin and triatin identified in our work and the two recently characterized *T. infestans* triplatin-1 and -2 [7] are shown in Fig. 2. Both triplatins are collagen-induced platelet-aggregation inhibitors that target the major collagen-signaling receptor glycoprotein VI and, consequently, inhibit platelet activation by collagen [7]. TiLipo33 clustered with triplatin-1 (84/90% identity/similarity), which is homolo-

Table 1
T. infestans salivary proteins identification by tandem mass spectrometry using MASCOT and MS BLAST methods

Spots[a]	Protein family members	Proposed functions	MASCOT identification					Identification by de novo sequencing and MS BLAST searches				pI[j]	Mr (kDa)[k]
			Significant hits[b]	Accession number[c]	Score[d]	Unique peptide no.[e]	Coverage (%)[f]	Significant hits[g]	Accession number[c]	Matched queries no.[h]	Coverage (%)[i]		
T. nfestans salivary proteins with unknown function and non-identified proteins													
75[l]	Unknown	Unknown	Ti_Triatox	Q45KX2	65	1	19	NI				7.3	31.5
165[l]	Unknown	Unknown	Ti_Triatox	Q45KX2	80	1	19	NI				8.0	19.4
192[l]	Unknown	Unknown	Ti_Triatox	Q45KX2	328	8	38	NI				5.0	16.2
83	Unknown	Unknown	NI					NI				5.3	30.9
201	Unknown	Unknown	NI					NI				5.6	14.4
260	Unknown	Unknown	NI					NI				9.4	11.7
269	Unknown	Unknown	NI					NI				8.5	9.9
T. infestans salivary proteins with blood-feeding putative functions													
45	ATPase	ATP binding and hydrolysis	Mitochondrial F1 ATP synthase α-chain [*A. fumigatus*]	Q4WC88	67	4	7	Mitochondrial ATPase α-s/u [*N. crassa*]	P37211	2	4.2	4.8	35.1
46	ATPase	ATP binding and hydrolysis	ADP, ATP carrier protein [*S. kluyveri*]	Q875Q6	105	2	6	Putative ATP synthase α-chain [*R. palustris*]	Q6NDD0	1	2.6	5.0	34.9
143	ATPase	ATP binding and hydrolysis	Mitochondrial ATP synthase β-chain [*G. zeae*]	Q4IEP6	289	4	10	Mitochondrial F1 ATP synthase β-s/u [*S. cerevisiae*]	P00830	4	8.4	9.0	21.9
51	Alkaline phosphatase	Phosphate hydrolysis	NI					Alkaline phosphatase L [*P. aeruginosa*]	P35482	1	3.5	9.7	34.4
167[l]	PBP	Phosphate transport	Periplasmic PBP [*R. palustris*]	Q6N0I2	138	2	10	ABC transporter PBP [*B. japonicum*]	Q89VF5	4	11.4	9.8	19.2
181[l]	PBP	Phosphate transport	Periplasmic PBP [*R. palustris*]	Q6N0I2	149	2	10	ABC transporter PBP [*B. japonicum*]	Q89VF5	6		8.0	17.8
192[l]	PBP	Phosphate transport	Periplasmic PBP [*R. palustris*]	Q6N0I2	98	1	5	Periplasmic PBP [*R. palustris*]	Q6N0I2	1	3.9	5.0	16.2
T. infestans salivary proteins with functions known to promote the blood-feeding													
77	Apyrase	ADP-induced platelet inhibitor	Ti_APY79	Q70GK8	141	3	6	Ti_APY79	Q70GK8	2	5.2	7.5	31.5
61	Triabin	Platelet inhibitor	TiLipo39	Q6UN99	85	1	10	TiLipo39	Q6UN99	2	10.1	5.1	32.6
75[l]	Triabin	Platelet inhibitor	NI					TiLipo33	Q6UNA0	2	14.9	7.3	31.5
114	Triabin	Platelet inhibitor	Ti_triatin	Q45KX3	772	14	37					8.9	28.5
								TiLipo37	Q6UNA1	3	14.0		
115	Triabin	Platelet inhibitor	Ti_triatin	Q45KX3	920	16	38	TiLipo39	Q6UN99	3	19.6	9.2	28.3
117[l]	Triabin	Platelet inhibitor	TiLipo39	Q6UN99	97	1	10	TiLipo39	Q6UN99	2	14.5	5.2	27.7
131	Triabin	Platelet inhibitor	Ni					TiLipo37	Q6UNA1	2	9.0	5.2	24.8
133[l]	Triabin	Platelet inhibitor	TiLipo39	Q6UN99	79	1	10	TiLipo39	Q6UN99	2	11.7	9.8	24.3
149	Triabin	Platelet inhibitor	NI					TiLipo37	Q6UNA1	3	15.7	8.4	21.3
150	Triabin	Platelet inhibitor	NI					TiLipo77	Q6UN98	3	14.0	9.0	21.1
151	Triabin	Platelet inhibitor	NI					TiLipo33	Q6UNA0	5	30.9	9.4	20.1
153[l]	Triabin	Platelet inhibitor	TiLipo33	Q6UNA0	91	1	9	TiLipo33	Q6UNA0	3	19.3	9.8	20.9
	Triabin	Platelet inhibitor	Ti_infestilin	Q45KX1	88	1	13						
164	Triabin	Platelet inhibitor	TiLipo33	Q6UNA0	87	1	9	TiLipo33	Q6UNA0	12	76.2	7.1	19.4
165[l]	Triabin	Platelet inhibitor	NI					TiLipo33	Q6UNA0	8	56.4	8.0	19.4
166[l]	Triabin	Platelet inhibitor	TiLipo39	Q6UN99	102	1	10					8.4	19.4
	Triabin	Platelet inhibitor	TiLipo33	Q6UNA0	88	1	9	TiLipo33	Q6UNA0	8	54.1		
167[l]	Triabin	Platelet inhibitor	TiLipo33	Q6UNA0	99	1	9	TiLipo33	Q6UNA0	7	45.9	9.8	19.2
168	Triabin	Platelet inhibitor	TiLipo33	Q6UNA0	247	2	20	TiLipo33	Q6UNA0	9	58.6	8.7	19.1

169	Triabin	Platelet inhibitor	TiLipo39	Q6UN99	115	1	10	NI				9.1	18.9
176[l]	Triabin	Platelet inhibitor	Ti_infestilin	Q45KX1	241	5	27					9.2	17.9
	Triabin	Platelet inhibitor	TiLipo39	Q6UN99	185	4	18	TiLipo39	Q6UN99	5	33.0		
	Triabin	Platelet inhibitor	Ti_triatin	Q45KX3	135	3	14						
177[l]	Triabin	Platelet inhibitor	TiLipo39	Q6UN99	177	4	18	TiLipo39	Q6UN99	6	40.2	8.6	17.9
	Triabin	Platelet inhibitor	Ti_infestilin	Q45KX1	108	2	16						
	Triabin	Platelet inhibitor	TiLipo33	Q6UNA0	104	1	11						
181[l]	Triabin	Platelet inhibitor	TiLipo33	Q6UNA0	128	1	11	TiLipo33	Q6UNA0	6	40.3	8.0	17.8
183[l]	Triabin	Platelet inhibitor	Ti_infestilin	Q45KX1	371/26	6	29	NI				9.6	17.5
	Triabin	Platelet inhibitor	TiLipo39	Q6UN99	181	4	18						
184	Triabin	Platelet inhibitor	TiLipo39	Q6UN99	281	6	25	TiLipo39	Q6UN99	9	59.8	8.6	17.5
185	Triabin	Platelet inhibitor	TiLipo39	Q6UN99	259	6	25	TiLipo39	Q6UN99	9	61.5	9.1	17.4
186[l]	Triabin	Platelet inhibitor	TiLipo39	Q6UN99	369	7	25	TiLipo39	Q6UN99	13	86.6	9.4	17.3
	Triabin	Platelet inhibitor	Ti_infestilin	Q45KX1	226	4	27						
187	Triabin	Platelet inhibitor	TiLipo39	Q6UN99	107	3	18	TiLipo39	Q6UN99	5	31.8	9.0	16.8
190	Triabin	Platelet inhibitor	TiLipo39	Q6UN99	174	4	22	TiLipo39	Q6UN99	4	29.6	9.4	16.7
197	Triabin	Platelet inhibitor	TiLipo39	Q6UN99	76	1	10	TiLipo39	Q6UN99	1	6.2	5.4	15.1
202[l]	Triabin	Platelet inhibitor	TiLipo39	Q6UN99	81	1	10					6.0	14.3
	Triabin	Platelet inhibitor						TiLipo33	Q6UNA0	2	13.3		
238[l]	Triabin	Platelet inhibitor	Ti_triatin	Q45KX3	351	7	18					9	15.1
	Triabin	Platelet inhibitor	TiLipo39	Q6UN99	133	3	18	TiLipo39	Q6UN99	5	30.7		
265	Triabin	Platelet inhibitor	TiLipo33	Q6UNA0	113	1	9	TiLipo33	Q6UNA0	3	18.8	8.7	10.8
267	Triabin	Platelet inhibitor	Ti_triatin	Q45KX3	513	11	45	NI				9.2	10.6
117[l]	Trialysin	Cell lysis	Ti_trialysin	Q8T0Z3	94	3	7	NI				5.2	27.7
121	Trialysin	Cell lysis	Ti_trialysin	Q8T0Z4	222	6	26	NI				5.0	27.4
133[l]	Trialysin	Cell lysis	Ti_trialysin	Q8T0Z3	76	3	5	NI				9.8	24.3
139	Trialysin	Cell lysis	Ti_trialysin	Q8T0Z3	360	7	19	NI				9.8	22.4

NI, non-identified protein; PBP, phosphate binding protein; Ti, *Triatoma infestans*; *A.*, *Aspergillus*; *B.*, *Bradyrhizobium*; *G.*, *Gibberella*; *N.*, *Neurospora*; *P.*, *Pseudomonas*; *R.*, *Rhodopseudomonas*; *S.*, *Saccharomyces*.

[a] Spot numbers correspond to the numbers indicated in Fig. 1.

[b] and (g) Protein identified with significant hits, respectively, via MASCOT and via MS BLAST.

[c] Accession number in SwissProt/TrEMBL.

[d] Probability Based Mowse Score of MASCOT software: $-10 \times \log(P)$, where P is the probability that the observed match is a random event.

[e] Number of unique peptide sequences identified via MASCOT.

[f] Coverage (%): percentage of predicted protein sequence covered by matched peptides via MASCOT.

[g] Protein identified with significant hits, respectively, via MASCOT and via MS BLAST.

[h] Number of unique peptide sequences identified via MS BLAST that had a significant sequence-alignment score superior or equal to 55.

[i] Coverage (%): percentage of predicted protein sequence covered by matched query sequences with an alignment score superior to 55% via MS BLAST according to [$\sum$positive queries (aa) $\times$ 100]/predicted protein (aa).

[j] Experimental isoelectric point of protein on gel.

[k] Experimental relative molecular mass of protein on gel.

[l] Spots probably containing more than one identified protein and could be present in two categories of *T. infestans* salivary proteins.

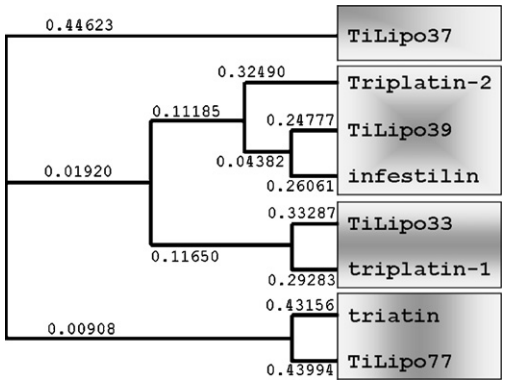

Fig. 2. Phylogenetic analysis of the *T. infestans* salivary triabin subfamily. Unrooted tree showing the sequence distance relationships between deposited members of the triabin subfamily. Numbers are branch lengths. Presumed clusters were boxed. Protein accession numbers used in this analysis are in Table 1.

gous to *T. pallidipennis* pallidin-2 (52/70% identity/similarity), another collagen-induced platelet-aggregation inhibitor [8]. On the other hand, both Tilipo39 and infestilin (68/78% identity/similarity) clustered with triplatin-2 (respectively, 71/81 and 73/80% identity/similarity). Finally, TiLipo77 and triatin formed another group (31/45% identity/similarity), while TiLipo37 was included in a separate branch. All of them are probably implicated in platelet-aggregation inhibition.

The data indicates that *T. infestans* saliva presents a diversity of lipocalin-like proteins that possibly act as anti-hemostatic factors during blood meal uptake as already reported for other triatomine bugs [36,42] and ticks [43,44]. Nevertheless, sequence variation within each major group of *R. prolixus* lipocalins was demonstrated to have important anti-hemostatic functional consequences and provides an excellent example of adaptive diversification of a single protein family in a specialized tissue [42].

The two *T. infestans* trialysin sequences were identified in four different spots. Trialysin is a pore-forming protein that lyses protozoan and bacterial cells indicating a role in the control of microorganism growth in the salivary glands as well as in the promotion of the blood-feeding process since it is able to permeabilize mammalian cells [45].

In addition, the protein spot 77 at 31.5 kDa matched *T. infestans* 79 kDa salivary apyrase precursor, an ADP collagen-induced platelet-aggregation inhibitor [16]. It could be a new apyrase form or just a proteolysis product. As a matter of fact, previous reports showed that *T. infestans* saliva apyrases are present in five different forms, namely TiAPY88, TiAPY82, TiAPY79, TiAPY68 and TiAPY67, with Mr of 88, 82, 79, 68 and 67 kDa, respectively [16]. The spots detected between 67 and 88 kDa on pH 3–10 2-DE gels (Fig. 1) could correspond to *T. infestans* salivary apyrases [16]. However, since they were in the basic p*I* region, their resolution was compromised by horizontal streaking. In order to obtain better resolution for such spots, we carried out 2-DE using a pH gradient from 6 to 11. In addition, immunoblotting using specific anti-apyrase antibodies was employed in order to locate apyrases in 2-DE gels as shown below.

3.2. Immunodetection analysis of TiAPY isoforms on alkaline 2-DE maps

The separation of basic proteins at good resolution by 2-DE is always a challenge due to intrinsic difficulties of isoelectric focusing in alkaline pH [46,47]. Here, to improve the separation of basic proteins over 45 kDa in 2-DE gels (Fig. 1), including all TiAPYs, we performed 2-DE in restricted pH range in alkaline conditions (pH 6–11). Different IEF conditions of basic salivary proteins were tested (data not shown). We found that the best separation of basic salivary proteins was achieved using the Multiphor II apparatus, rehydration of alkaline IPG strips with rehydration buffer without sample prior to IEF and anodic sample application using the paper-bridge method [30] plus an electrode pad embedded in DTT solution near the cathode. Thus, the horizontal streaking in the region of high apparent molecular masses observed in Fig. 1 disappeared in the alkaline 2-DE gels (Fig. 4A and B). To determine if the spots between 67 and 88 kDa were isoforms of the five apyrases previously described [16], we employed Western blotting, since specific antisera against TiAPY88, TiAPY82 and TiAPY79 are readily available.

Proteins from secreted saliva and proteins extracted from gland pairs that are named according to Barth [48] as D1 (principal), D2 (Supplementary) and D3 (accessory). Such nomenclature is still in use [40]. The gland contents were subjected to SDS-PAGE (Fig. 3A) followed by immunoblotting using specific anti-apyrase sera (Fig. 3B–D). It was observed that each anti-apyrase serum specifically labeled one protein band at the expected molecular mass in secreted saliva as well in the lumen of the salivary gland pair D2 (Fig. 3). No labeling was detected in gland pairs D1 and D3. Previous work found apyrases mainly in the lumen of pair D1 [17]. Further experiments should be done to explain such apparently contradictory results. When the developing time of the immunodetection was increased, the bands of the other apyrases became visible, including TiAPY68 and TiAPY67 for which we did not produce antibody (Fig. 3), presumably because conserved sequence domains are shared between different TiAPY forms [16].

In the alkaline 2-DE gel conditions, each antiserum specifically labeled some spots at the expected relative molecular masses corresponding to apyrase bands in SDS-PAGE (Fig. 4). TiAPY88, TiAPY79, TiAPY68 and TiAPY67 showed at least two isoforms each, always detectable both on silver-stained and Western-blotted gels. Interestingly, TiAPY82 and their potential isoforms visualized in Fig. 4B were not always present in alkaline 2-DE gels (Fig. 4A) depending on the pool of *T. infestans* saliva used. Although both silver-stained gels and immunoblots suggested the existence of isoenzymes of each apyrase member, we employed the same MS/MS peptide sequencing technique described above to confirm the identity of such isoforms.

3.3. Validation of TiAPY isoforms by MS/MS

Fifteen anti-apyrase cross-reacting spots were characterized by nanoLC–MS/MS, as described above. Altogether, de novo sequencing identified more apyrase isoforms than conventional MASCOT searching. From a total of 15 analyzed spots, 13

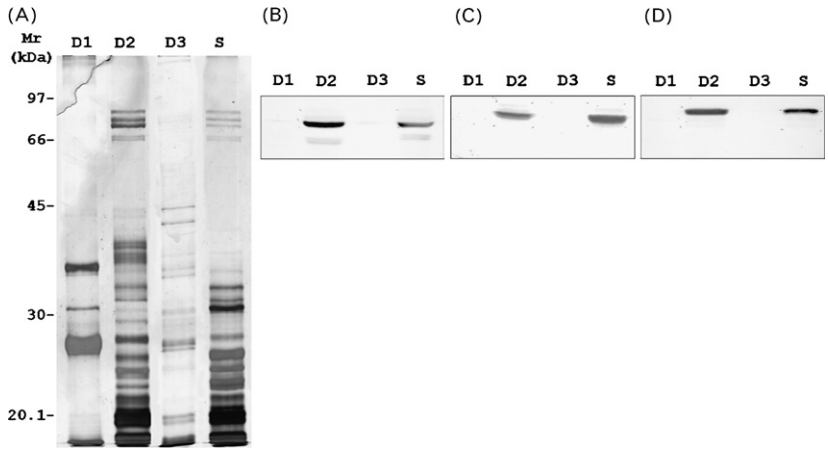

Fig. 3. Glandular localization of TiAPY. Proteins from gland pair D1 (lanes D1) and gland pair D2 (lanes D2) and gland pair D3 (lanes D3) and crude secreted saliva (lanes S) were separated by 10% SDS-PAGE and silver-stained (A). TiAPY localization analyses were performed by Western blotting using anti-TiAPY79 serum (B), anti-TiAPY82 serum (C) and anti-TiAPY88 serum (D).

were positively identified by MASCOT including one borderline identification that was confirmed by MS BLAST validation procedure as described in Ref. [49]. Sequence-similarity searches allowed us to identify all 15 isoforms including the two spots that could not be identified by MASCOT. The number of unique peptides matched by sequence-similarity searches was, in most of the cases, higher than in MASCOT searches (Table 2 and Supplementary Table 2).

Alignments between all sequence proposals obtained by de novo MS/MS against the only available sequence of *T. infestans* 79 kDa salivary apyrase (EMBL accession number AJ581749) confirmed high sequence similarity (Fig. 5). As expected, the

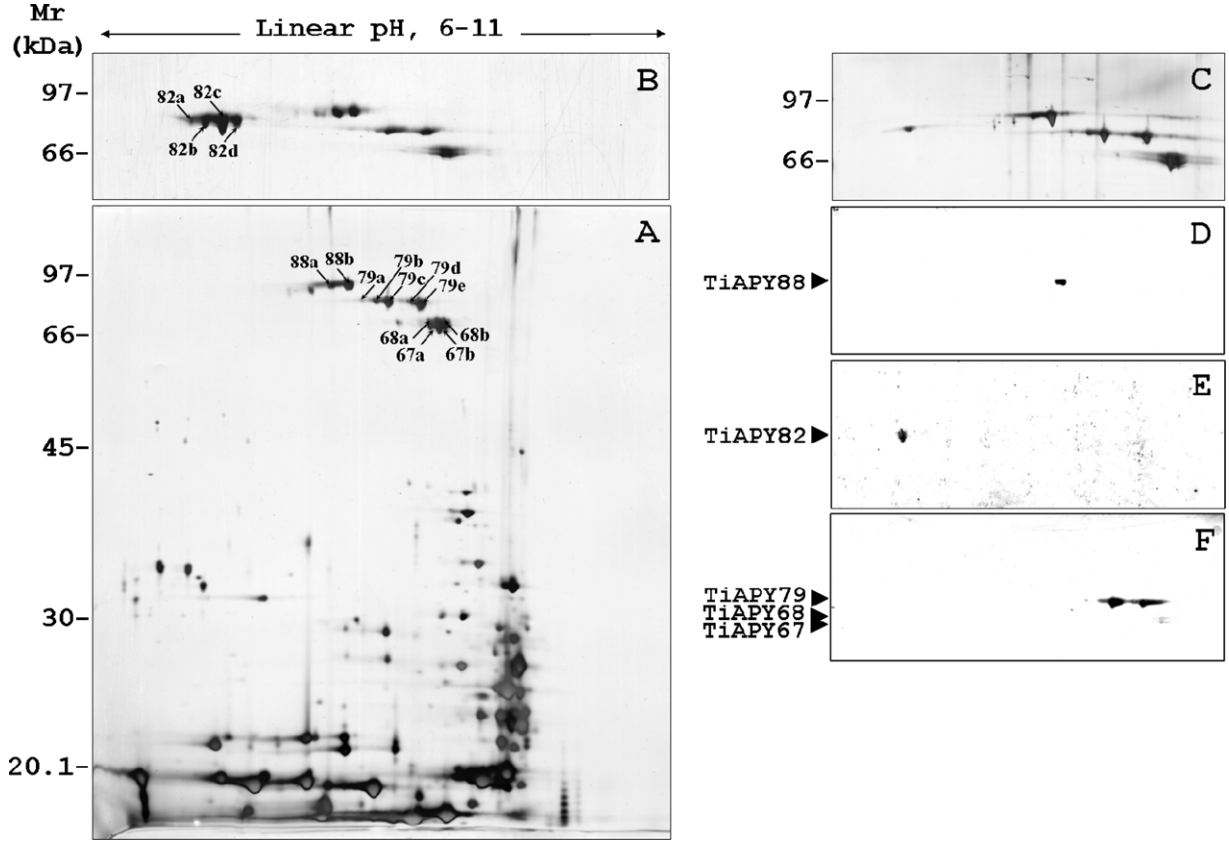

Fig. 4. TiAPY localization and immunodetection of *T. infestans* secreted saliva on alkaline 2-DE map. 2-DE gels were performed under denaturing conditions using 6–11 linear IPG strips in IEF and 10% SDS-PAGE in second dimension. The sample amount was 240 μg of salivary proteins. The gels were silver-stained, entire 2-DE gel (A), and (B and C) restricted up-region gels containing TiAPY spots, or Western blotted on nitrocellulose membrane using anti-TiAPY88 serum (D), anti-TiAPY82 serum (E) and anti-TiAPY79 serum (F). TiAPY68 and TiAPY67 were faintly revealed with anti-TiAPY79 serum (F). Spot numbers on (A and B) correspond to MS/MS identified TiAPY isoforms shown in Table 2.

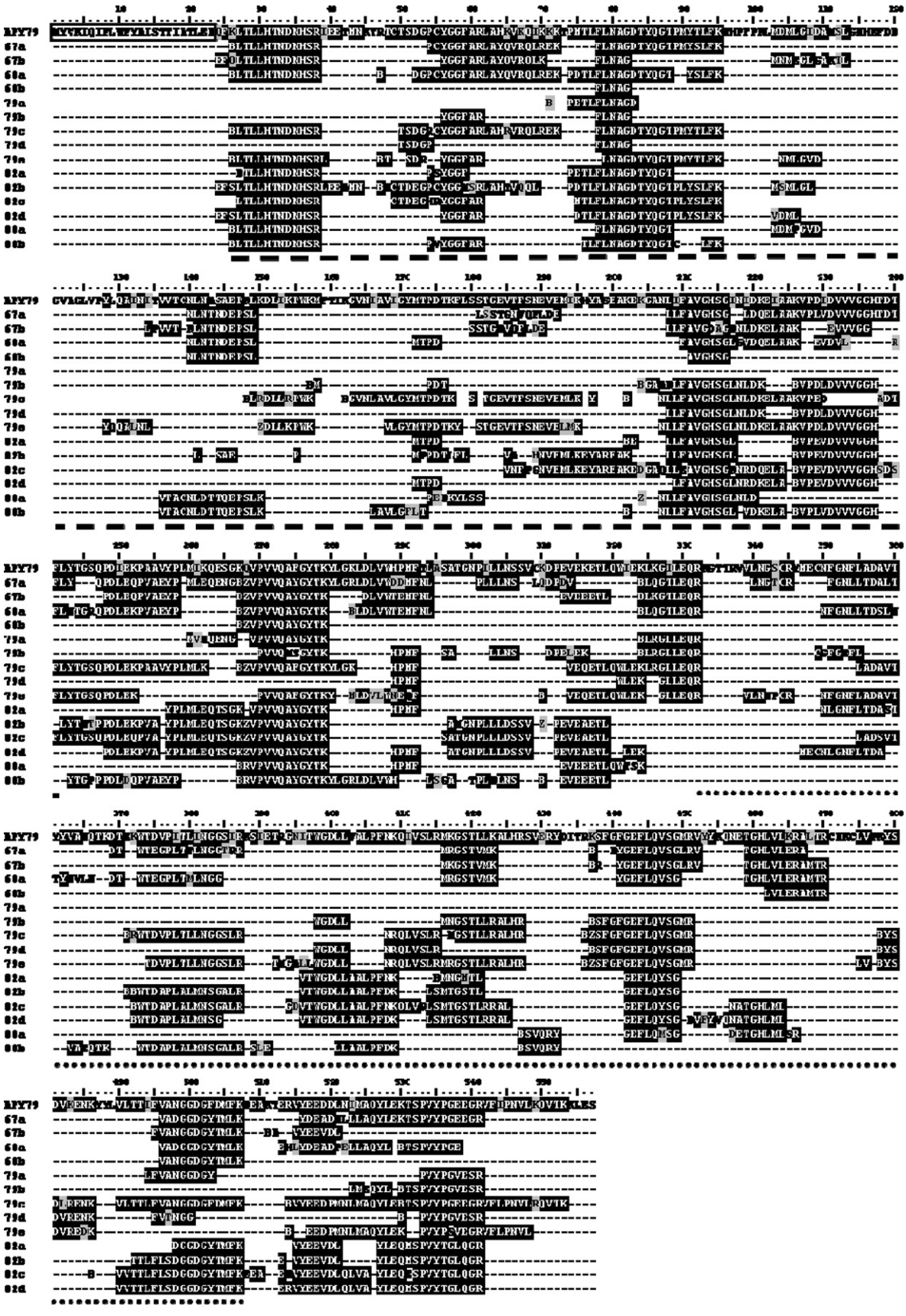

Fig. 5. Amino acid sequence alignment of sequenced peptides from all apyrase isoforms with APY79 precursor. The alignment was performed by ClustalW. Conserved residues are shaded in black, conserved substitutions are shaded in grey. The predicted signal peptide of 23 aa is boxed. The two conserved domains are indicated by a dashed line (Calcineurin-like phosphoesterase), and a dotted line (5′-nucleotidase).

Table 2
T. infestans apyrase isoforms identified by tandem mass spectrometry using MASCOT and MS BLAST methods

Apyrase form	Apyrase isoform[a]	MASCOT identification			Identification by de novo sequencing and MS BLAST searches		pI[g]	Mr (kDa)[h]
		MOWSE score[b]	Unique peptide number[c]	Coverage (%)[d]	Matched queries number (score ≥55)[e]	Coverage (%)[f]		
67	67a	105	2	4	14	26.8	8.9	67.3
	67b	105	3	5	4	8.4	8.9	67.9
68	68a	105	2	4	8	16.0	8.8	70.6
	68b	84	2	4	2	4.1	8.9	71.1
79	79a	NI	NI	NI	2	3.8	8.2	80.4
	79b	451	12	21	6	12.6	8.4	80.4
	79c	1427	27	45	21	47.2	8.5	79.9
	79d	389	11	18	4	8.8	8.7	79.9
	79e	1438	32	44	18	38.1	8.7	78.6
82	82a	NI	NI	NI	9	17.6	6.6	83.7
	82b	80	2	3	14	27.7	6.8	83.3
	82c	92	4	3	15	31.8	6.9	82.4
	82d	38[i]	2	1	15	30.7	7.1	83.1
88	88a	87	1	2	5	10.2	8.1	89.0
	88b	70	1	2	9	18.1	8.0	88.8

NI, non-identified protein.
[a] Apyrase isoform names correspond to the spots numbers indicated in Fig. 4.
[b] Probability Based Mowse Score of MASCOT software: $-10 \times \log(P)$, where P is the probability that the observed match is a random event.
[c] Number of unique tryptic peptide sequences identified via MASCOT.
[d] Coverage (%): percentage of predicted protein sequence covered by matched peptides via MASCOT.
[e] Number of unique peptide sequences identified via MS BLAST that had a significant sequence-alignment score superior to 55%.
[f] Coverage (%): percentage of deposited TiAPY79 sequence covered by matched query sequences with a alignment score superior to 55% via MS BLAST according to [$\sum$positive queries (aa) × 100]/predicted protein (aa).
[g] Experimental isoelectric point of protein on gel.
[h] Experimental relative molecular mass of protein on gel.
[i] Indicates that the score reported is not statistically significant.

N-terminal region (amino acid residues 1–23), corresponding to the predicted signal peptide, was not found in MS/MS analyses (Fig. 5).

Peptide sequences from the apyrase isoforms differed in few amino acid residues, indicating that such isoforms may have been originated from sequence polymorphism as reported for other proteins of insect and spider species [24,50]. In fact, *T. infestans* was proposed to have a multi-gene apyrase family with, at least, three to five loci since 88 and 82 kDa apyrases are absent in some individuals [16]. Moreover 2-DE saliva proteome profiles are similar regarding the apyrase isoforms patterns if they come from an insect saliva pool or a single individual (data not shown). It is possible, however, that post-translational modifications might also be a source of apyrase heterogeneity, since the five isoforms were shown to be *N*-glycosylated in Ref. [16].

To test if all isoforms were associated with apyrase activity, we tried to perform in-gel activity assay, as previously described for 1-DE or IEF separately [18], but modified for entirely native 2-DE. Diffuse 2-DE apyrase activity was found (data not shown), but no conclusive results were possible to be drawn so far, probably due to apyrase oligomerization that occurs under native conditions [18]. However, it seems to corroborate oligomerization-dependent 5′-nucleotidase activity in vitro.

4. Conclusions

As bloodsucking arthropods, haematophagous *Triatomine* bugs produce a diversity of compounds of biotechnological or medical perspective. Pharmacological substances in their saliva counteract vertebrate host hemostatic events, such as coagulation, vasoconstriction and platelet aggregation, and modulate vertebrate immune-response [41].

Here we report that *T. infestans* saliva proteome contain mainly platelet-aggregation inhibitors that belong to lipocalin and apyrase families. The apparent redundancy of proteins with predicted and known anti-platelet function belonging to same families should represent enhanced highly specific mechanism activated as an early response to reduce the platelet aggregation of the prey blood in order to facilitate feeding. On the other hand, the existence of various proteins and isoforms related to anti-hemostatic activity in bug saliva could reside in an evolutionary adaptation for the insect to drive a great success in the bloodsucking. The *T. infestans* crude saliva seems to differ from other insect and tick saliva by apyrase diversity and abundance. It would be interesting to characterize apyrase isoforms separately, in order to compare their affinity to the ligands ATP and ADP in different environmental conditions (e.g. pH and temperature), to clarify the reason for protein redundancy. In addition, the new identified proteins with unknown or putative

functions may play important roles in blood meal and deserve future functional characterization studies. These proteins found in *T. infestans* saliva have potential biotechnological applications and can eventually be tested as anti-thrombotic agents and even as targets of a cocktail-vaccine to prevent *Trypanosoma cruzi* transmission.

Acknowledgments

We thank Dr. Jaime Paba for relevant technical advices and Nuno Domingues for technical assistance on amino acid analyses. We wish to thank Prof. Jaime M. Santana for the kind gift of the anti-TiAPY antibodies, his advices and extremely helpful position for the accomplishment of this work. This work was supported by a post-doctoral fellowship from Conselho Nacional de Desenvolvimento Científico e Tecnológico (CNPq), Brazil, attributed to Dr Sébastien Charneau, and by Grants from Fundação de Empreendimentos Científicos e Tecnológicos (FINATEC), Brazil and Fundação de Apoio à Pesquisa do Distrito Federal (FAPDF, PRONEX Program), Brazil.

Appendix A. Supplementary data

Supplementary data associated with this article can be found, in the online version, at doi:10.1016/j.ijms.2007.05.004.

References

[1] WHO, World Health Organ. Tech. Rep. Ser. 905, 2002, i–vi, p. 1 (back cover).
[2] M.P. Barrett, R.J. Burchmore, A. Stich, J.O. Lazzari, A.C. Frasch, J.J. Cazzulo, S. Krishna, Lancet 362 (2003) 1469.
[3] B.B. Andrade, C.R. Teixeira, A. Barral, M. Barral-Netto, An. Acad. Bras. Cienc. 77 (2005) 665.
[4] R.C. Jin, B. Voetsch, J. Loscalzo, Microcirculation 12 (2005) 247.
[5] C.J. Schofield, Ann. Soc. Belg. Med. Trop. 65 (Suppl. 1) (1985) 149.
[6] M.H. Pereira, N.F. Gontijo, A.A. Guarneri, M.R. Sant'anna, L. Diotaiuti, Trends Parasitol. 22 (2006) 516.
[7] A. Morita, H. Isawa, Y. Orito, S. Iwanaga, Y. Chinzei, M. Yuda, Febs J. 273 (2006) 2955.
[8] C. Noeske-Jungblut, J. Kratzschmar, B. Haendler, A. Alagon, L. Possani, P. Verhallen, P. Donner, W.D. Schleuning, J. Biol. Chem. 269 (1994) 5050.
[9] C. Noeske-Jungblut, B. Haendler, P. Donner, A. Alagon, L. Possani, W.D. Schleuning, J. Biol. Chem. 270 (1995) 28629.
[10] P. Fuentes-Prior, C. Noeske-Jungblut, P. Donner, W.D. Schleuning, R. Huber, W. Bode, Proc. Natl. Acad. Sci. U.S.A. 94 (1997) 11845.
[11] I.M. Francischetti, J.M. Ribeiro, D. Champagne, J. Andersen, J. Biol. Chem. 275 (2000) 12639.
[12] I.M. Francischetti, J.F. Andersen, J.M. Ribeiro, Biochemistry 41 (2002) 3810.
[13] D.R. Flower, Biochem. J. 318 (Pt 1) (1996) 1.
[14] J.J. Sarkis, J.A. Guimaraes, J.M. Ribeiro, Biochem. J. 233 (1986) 885.
[15] J.M. Ribeiro, E.S. Garcia, Experientia 37 (1981) 384.
[16] E. Faudry, S.P. Lozzi, J.M. Santana, M. D'Souza-Ault, S. Kieffer, C.R. Felix, C.A. Ricart, M.V. Sousa, T. Vernet, A.R. Teixeira, J. Biol. Chem. 279 (2004) 19607.
[17] E. Faudry, P.S. Rocha, T. Vernet, S.P. Lozzi, A.R. Teixeira, Insect Biochem. Mol. Biol. 34 (2004) 1051.
[18] E. Faudry, J.M. Santana, C. Ebel, T. Vernet, A.R. Teixeira, Biochem. J. 396 (2006) 509.
[19] A.J. Liska, A. Shevchenko, Proteomics 3 (2003) 19.
[20] K.G. Standing, Curr. Opin. Struct. Biol. 13 (2003) 595.
[21] R.S. Johnson, M.T. Davis, J.A. Taylor, S.D. Patterson, Methods 35 (2005) 223.
[22] A.J. Liska, A. Shevchenko, Trends Anal. Chem. 22 (2003) 291.
[23] A.J. Liska, A.V. Popov, S. Sunyaev, P. Coughlin, B. Habermann, A. Shevchenko, P. Bork, E. Karsenti, Proteomics 4 (2004) 2707.
[24] A. Shevchenko, M.M. de Sousa, P. Waridel, S.T. Bittencourt, M.V. de Sousa, J. Proteome Res. 4 (2005) 862.
[25] A.J. Liska, A. Shevchenko, U. Pick, A. Katz, Plant Physiol. 136 (2004) 2806.
[26] R.A. Guercio, A. Shevchenko, J.L. Lopez-Lozano, J. Paba, M.V. Sousa, C.A. Ricart, Proteome Sci. 4 (2006) 11.
[27] D.E. Kalume, M. Okulate, J. Zhong, R. Reddy, S. Suresh, N. Deshpande, N. Kumar, A. Pandey, Proteomics 5 (2005) 3765.
[28] J.C. Sanchez, V. Rouge, M. Pisteur, F. Ravier, L. Tonella, M. Moosmayer, M.R. Wilkins, D.F. Hochstrasser, Electrophoresis 18 (1997) 324.
[29] J. Paba, J.M. Santana, A.R. Teixeira, W. Fontes, M.V. Sousa, C.A. Ricart, Proteomics 4 (2004) 1052.
[30] F. Sabounchi-Schutt, J. Astrom, I. Olsson, A. Eklund, J. Grunewald, B. Bjellqvist, Electrophoresis 21 (2000) 3649.
[31] A. Shevchenko, M. Wilm, O. Vorm, M. Mann, Anal. Chem. 68 (1996) 850.
[32] A. Frank, P. Pevzner, Anal. Chem. 77 (2005) 964.
[33] A. Shevchenko, S. Sunyaev, A. Liska, P. Bork, A. Shevchenko, Methods Mol. Biol. 211 (2003) 221.
[34] B. Habermann, J. Oegema, S. Sunyaev, A. Shevchenko, Mol. Cell. Proteomics 3 (2004) 238.
[35] N. Campostrini, L.B. Areces, J. Rappsilber, M.C. Pietrogrande, F. Dondi, F. Pastorino, M. Ponzoni, P.G. Righetti, Proteomics 5 (2005) 2385.
[36] J.M. Ribeiro, J. Andersen, M.A. Silva-Neto, V.M. Pham, M.K. Garfield, J.G. Valenzuela, Insect Biochem. Mol. Biol. 34 (2004) 61.
[37] J.M. Ribeiro, B. Arca, F. Lombardo, E. Calvo, V.M. Phan, P.K. Chandra, S.K. Wikel, BMC Genomics 8 (2007) 6.
[38] M.A. Packham, J.F. Mustard, Semin. Thromb. Hemost. 31 (2005) 129.
[39] J.F. Andersen, J.M. Ribeiro, Biochemistry 45 (2006) 5450.
[40] M.M. Reis, R.M. Meirelles, M.J. Soares, Tissue Cell 35 (2003) 393.
[41] J.M. Ribeiro, I.M. Francischetti, Annu. Rev. Entomol. 48 (2003) 73.
[42] J.F. Andersen, N.P. Gudderra, I.M. Francischetti, J.M. Ribeiro, Arch. Insect Biochem. Physiol. 58 (2005) 97.
[43] G.C. Paesen, P.L. Adams, P.A. Nuttall, D.L. Stuart, Biochim. Biophys. Acta 1482 (2000) 92.
[44] S. Sangamnatdej, G.C. Paesen, M. Slovak, P.A. Nuttall, Insect Mol. Biol. 11 (2002) 79.
[45] R. Amino, R.M. Martins, J. Procopio, I.Y. Hirata, M.A. Juliano, S. Schenkman, J. Biol. Chem. 277 (2002) 6207.
[46] K. Pennington, E. McGregor, C.L. Beasley, I. Everall, D. Cotter, M.J. Dunn, Proteomics 4 (2004) 27.
[47] G. Chinnasamy, C. Rampitsch, Biochim. Biophys. Acta 1764 (2006) 641.
[48] R. Barth, Mem. Inst. Oswaldo Cruz (1954) 517.
[49] N. Wielsch, H. Thomas, V. Surendranath, P. Waridel, A. Frank, P. Pevzner, A. Shevchenko, J. Proteome Res. 5 (2006) 2448.
[50] L.F. Machado, S. Laugesen, E.D. Botelho, C.A. Ricart, W. Fontes, K.C. Barbaro, P. Roepstorff, M.V. Sousa, Proteomics 5 (2005) 2167.